

# IMPACT OF AGGREGATE SHAPE ON DRYING SHRINKAGE CRACKING IN CONCRETE: A THREE-DIMENSIONAL HYDRO-MECHANICAL PERIDYNAMIC MODEL

Yu SUN\*, Yun JIA<sup>†</sup>, Jean-Philippe CARLIER<sup>†</sup> AND Thomas ROUGELOT<sup>†</sup>

\* UMR 9013 - LaMcube - Laboratoire de Mecanique, Multiphysique, Multi-echelle, University of Lille, CNRS, Centrale Lille  
F-59000, Lille, France  
e-mail: yu.sun@univ-lille.fr

<sup>†</sup>UMR 9013 - LaMcube - Laboratoire de Mecanique, Multiphysique, Multi-echelle, University of Lille, CNRS, Centrale Lille  
F-59000, Lille, France

**Key words:** Hydro-Mechanical model, Peridynamic method, Inclusion shape, Drying shrinkage, Concrete fracture

**Abstract.** The crack evolution in concrete under drying conditions is significantly influenced by the shape of aggregates. This study presents a fully coupled three-dimensional hydro-mechanical peridynamic (PD) meso-scale model for partially saturated porous media to simulate crack formation in cementitious materials during drying shrinkage. Simulations were conducted on concrete samples with different aggregate shapes, including regular polyhedron (e.g., hexahedron, octahedron, dodecahedron, and icosahedron) and spheres. Results indicated that aggregates with lower sphericity led to higher stress concentrations and an increased formation of fine internal cracks. In contrast, aggregates with higher sphericity, such as spheres, produced a more uniform damage distribution, with fewer surface cracks. Damage analysis demonstrated that the sphericity of aggregates influenced early surface damage and denser crack networks, while higher sphericity in aggregates reduced the overall volume of internal cracks. The evolution of internal cracks over time underscored the sensitivity of the concrete matrix's mechanical response to aggregate morphology. This fully coupled hydro-mechanical PD model enhances our understanding of fracture behavior in concrete under drying conditions and underscores the critical role of aggregate shape in crack development. The insights gained from this study support optimized aggregate selection and improved structural design strategies to minimize drying shrinkage damage, contributing to the durability of concrete structures.

## 1 INTRODUCTION

Concrete is a widely used material in engineering applications, valued for its versatility and strength. However, its susceptibility to cracking, particularly due to drying shrinkage, remains a critical challenge for maintaining structural integrity. Drying shrinkage results from complex hydro-mechanical processes, such as capillary tension, surface energy

changes, and water migration, which induce internal stresses and lead to crack formation [1].

Aggregate properties, especially shape, significantly influence the distribution and intensity of these shrinkage-induced stresses [2]. While traditional numerical methods like the Finite Element Method (FEM) and Discrete Element Method (DEM) are widely employed for modeling concrete behavior, they have inher-

ent limitations in capturing crack initiation and propagation, especially in heterogeneous materials like concrete [3, 4]. FEM relies on predefined meshes and requires additional criteria for simulating discontinuities such as cracks, which complicates the analysis of crack branching and interaction. DEM, although capable of handling discrete particles, struggles with computational efficiency and accurate representation of the continuum behavior of the cement matrix at the meso-scale.

To overcome these challenges, this study employs a three-dimensional hydro-mechanical peridynamic model. Unlike FEM and DEM, peridynamics inherently accommodates discontinuities without requiring additional criteria, enabling seamless simulation of crack initiation and propagation [5]. This non-local method considers interactions over a finite distance, making it particularly suitable for capturing the complex interactions between aggregates and the cement matrix at the meso-scale [6].

## 2 Hydro-mechanical bond-based peridynamic model for cementitious material

### 2.1 Classic formulations

Peridynamics is a non-local continuum theory that effectively addresses challenges associated with structural discontinuities, which traditional continuum mechanics cannot handle. Unlike conventional numerical methods, in peridynamics, a material point inside a body interacts with other points within a specific range termed the "horizon  $\delta$ ," as shown in Fig. 1. The bond between two material points  $\mathbf{x}$  and  $\mathbf{x}'$  is expressed by a response function  $\mathbf{f}$ , which contains all the constitutive properties of the material point.

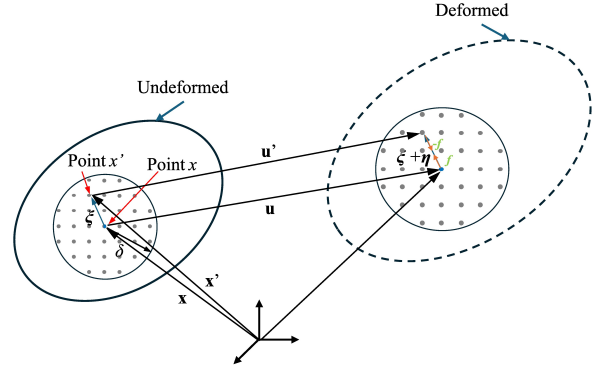


Figure 1: Principle of BB-PD theory in reference and deformed configuration

As derived by Silling (2000) [5], the peridynamic equation of motion at a reference position of  $\mathbf{x}$  and time  $t$  is given as

$$\rho(\mathbf{x})\ddot{\mathbf{u}}(\mathbf{x}, t) = \int_H \mathbf{f}(\mathbf{x}' - \mathbf{x}, \mathbf{u}' - \mathbf{u})dV + \mathbf{b}(\mathbf{x}, t) \quad (1)$$

where  $\rho$  is the mass density of material point in the reference configuration;  $\ddot{\mathbf{u}}$  is the acceleration quantity vector;  $\mathbf{b}$  is a prescribed body force density field;  $\mathbf{u}'$  and  $\mathbf{u}$  represent the displacements of the point  $\mathbf{x}'$  and the point  $\mathbf{x}$ , respectively;  $H$  is the neighborhood domain of the point  $\mathbf{x}$ . In three-dimensional (3D) problems, this domain is usually taken as a sphere. The horizon region centered at  $\mathbf{x}$  is defined by:

$$H = H(\mathbf{x}, \delta) = \{\mathbf{x}' \in R : \|\mathbf{x}' - \mathbf{x}\| \leq \delta\} \quad (2)$$

The response function  $\mathbf{f}$ , that defines the force between two material points, is written as

$$\mathbf{f} = cs \frac{\mathbf{y}' - \mathbf{y}}{\|\mathbf{y}' - \mathbf{y}\|} \quad (3)$$

where  $\mathbf{y}$  is the position of the material point  $\mathbf{x}$  in the deformed configuration equaling  $\mathbf{y} = \mathbf{x} + \mathbf{u}$ . The stretch  $s$  between the material point is defined as

$$s = \frac{\|\mathbf{y}' - \mathbf{y}\| - \|\mathbf{x}' - \mathbf{x}\|}{\|\mathbf{x}' - \mathbf{x}\|} \quad (4)$$

The material parameter (bond constant)  $c$  is the micro modulus, in 3D, which is expressed as

$$c = \frac{12E}{\pi\delta^4} \quad (5)$$

where  $E$  is the elastic modulus of the material.

## 2.2 Fluid flow field

Based on Darcy's law, which is used to describe the fluid flow in the porous medium, the governing equations for a single-phase fluid flow in concrete can be described as

$$\frac{\partial(\rho_f\beta)}{\partial t} = -\nabla \cdot (\rho_f\mathbf{v}) + q_f \quad (6)$$

where  $\beta$  is the variation in the water content,  $\rho_f$  is the density of the fluid,  $q_f$  is the mass of fluid produced per unit volume per unit time, and  $\mathbf{v}$  is the fluid velocity. As derived by Biot (1941) [7], Eq. (6) can be rewritten for constant material properties as

$$\frac{1}{Q_b} \frac{\partial P}{\partial t} = \frac{k_p}{\mu_v} \nabla^2 P - \alpha \frac{\partial \theta}{\partial t} + \frac{q_f}{\rho_f} \quad (7)$$

where  $P$  is the fluid pressure;  $k_p$  is the permeability of the porous medium;  $\mu_v$  is the fluid viscosity;  $\alpha$  and  $\theta$  represent the Biot parameter and the change in volume, respectively.  $Q_b$  is the Biot modulus for partially saturated porous medium and can be expressed as

$$\frac{1}{Q_b} = \frac{S_l^2(b - \phi)}{K_s} + \frac{S_l\phi}{K_f} - \phi \frac{\partial S_l}{\partial p_c} \quad (8)$$

where  $K_s$  and  $K_f$  are the bulk modulus of solid and fluid, respectively;  $\phi$  is the porosity. Furthermore, the water saturation ( $S_l$ ) has a relationship with the capillary pressure ( $p_c$ ) through the water retention curve. In this study, the widely used equation proposed by van Genuchten [8] is adopted:

$$S_l = S_l^r + (1 - S_l^r)[1 + (\epsilon p_c)^n]^{-m} \quad (9)$$

where  $S_l^r$  is the residual saturation degree;  $\epsilon$  is a scaling factor;  $m$  and  $n$  are two parameters and

can be calibrated by experimental data. The relative permeability of partially saturated porous medium is defined by the following function:

$$k_r = \sqrt{S_l} \left[ 1 - \left( 1 - S_l^{1/m} \right)^m \right]^2 \quad (10)$$

In 3D, the relation between PD permeability  $k_p$  and the permeability  $k$  for porous medium is given by

$$k_p = \frac{6k}{\pi\mu_v\delta^4} \quad (11)$$

## 2.3 Peridynamic equation of motion in the cementitious material

By using the analogy between poroelasticity and thermoelasticity, the peridynamic equation of motion of a material point at  $x$  can be modified as

$$\rho(\mathbf{x})\ddot{\mathbf{u}}(\mathbf{x}, t) = \int_H c\psi(\mathbf{x}, \mathbf{x}', t)(s - S_l\alpha\gamma \frac{P(\mathbf{x}', t) + P(\mathbf{x}, t)}{2}) \frac{\mathbf{y}' - \mathbf{y}}{\|\mathbf{y}' - \mathbf{y}\|} dV + \mathbf{b}(\mathbf{x}, t) \quad (12)$$

where  $\psi(\mathbf{x}, \mathbf{x}', t)$  is the state function of bonds;  $\gamma$  is the coefficient of fluid pore pressure defined as

$$\gamma = \frac{(1 - 2\nu)}{E} (3D) \quad (13)$$

with  $\nu$  representing the Poisson's ratio. The state function of the interacting bond in a horizon can be defined as follows:

$$\psi(\mathbf{x}, \mathbf{x}', t) = \begin{cases} 0, & s \geq s_0 \\ 1, & s < s_0 \end{cases} \quad (14)$$

where  $\psi(\mathbf{x}, \mathbf{x}', t)$  equaling 0 means that the bond is broken, while  $\psi(\mathbf{x}, \mathbf{x}', t)$  equaling 1 means that the bond is intact;  $s_0$  is the critical stretch of bonds, which can be obtained by the energy release rate  $G_0$  of macroscopic material:

$$s_0 = \sqrt{\frac{5G_0}{6E\delta}} \quad (15)$$

In PD theory, the damage at a material point is calculated based on the ratio of broken bonds to the total number of bonds within the horizon. Thus, the global damage function of material points is written as

$$D(\mathbf{x}, t) = 1 - \frac{\int_H \psi(\mathbf{x}, \mathbf{x}', t) dV}{\int_H dV} \quad (16)$$

### 3 Numerical discretization and implementation

#### 3.1 Spatial discretization

Based on PD theory, the computational model is discretized into regularly spaced particles, transforming the continuous medium into a finite grid with size  $\Delta x$ . By assigning each material point  $\mathbf{x}_i$  a volume  $\Delta V_i$ , the hydromechanical BB-PD integral equations can be approximated. The collection of PD material points  $\mathbf{x}_j$  lying within the neighborhood of  $\mathbf{x}_i$ , defined by the horizon  $\delta$ , is expressed as

$$H_i := \mathbf{x}_j \mid \mathbf{x}_j \neq \mathbf{x}_i, \mathbf{x}_j - \mathbf{x}_i \leq \delta \quad (17)$$

Therefore, the discretized hydro-mechanical BB-PD equations for the material point  $\mathbf{x}_i$  can be written as follows:

$$\rho(\mathbf{x}_i) \ddot{\mathbf{u}}(\mathbf{x}_i, t) = \sum_{\mathbf{x}_j \in H_i}^N c_{ij} \psi_{ij} (s_{ij} - S_l \alpha \gamma) \frac{P(\mathbf{x}_i, t) + P(\mathbf{x}_j, t)}{2} \frac{\mathbf{y}_j - \mathbf{y}_i}{\|\mathbf{y}_j - \mathbf{y}_i\|} \Delta V_i + \mathbf{b}(\mathbf{x}_i, t) \quad (18)$$

A previous study has demonstrated the accuracy of the PD method for coupled hydro-mechanical applications by comparing it with the FEM method [9].

### 4 Meso-scale modeling for concrete with aggregates of different shapes

#### 4.1 Parameter calibration

Calibration of model parameters is essential for ensuring the accuracy and reliability of the final simulation results. The simulation parameters are categorized into mechanical

and hydraulic groups. The mechanical parameters of cement paste were calibrated based on the stress-strain curve obtained from the uniaxial compression tests previously conducted on CEM II 32.5 cement cylinder sample. The mechanical behavior of the aggregate is assumed to be elastic. Table 1 summarizes the material parameters used in this study. Based on the experimental data of Rougelot et al. [10], the following parameters are adopted:  $S_l^r = 0$ ,  $\epsilon = 2.09\text{E-}8$ ,  $n = 1.9$ ,  $m = 0.47$ . The function of  $S_l$  can be expressed as:

$$S_l = [1 + (2.09 \times 10^{-8} p_c)^{1.9}]^{-0.47} \quad (19)$$

**Table 1:** Material parameters used in the simulation

Parameters	Cement	Aggregate
Elastic modulus E(GPa)	15	68
Poisson's ratio $\nu$	0.25	0.25
Energy release rate $G_0$ (N/mm)	0.03	0.5
Density $\rho$ (kg/m <sup>3</sup> )	1530	2500
Porosity $\phi$	0.35	-
Biot coefficient $\alpha$	0.63	-
The fluid viscosity (Pas)	1E-03	-
The permeability $k$ (mm <sup>2</sup> )	1E-14	-

#### 4.2 Three-dimensional Meso-scale model generation and boundary condition

Accurate meso-structure modeling is essential for understanding cementitious composites, which typically include a cement matrix, aggregates, and an interfacial transition zone (ITZ) [11]. The construction of three-dimensional meso-structures often considers three aggregate-related factors: (1) volume fraction, generally 30%-50% in normal concrete [12] (40% here); (2) gradation, referring to aggregate size and distribution, assumed uniform to reduce its effects; and (3) shape, commonly generated by mathematical random methods [13] or derived from scans of real aggregates [14].

The procedure begins with generating the cement matrix as the base for the meso-structure.

Aggregates are then placed using a 'Generate-and-Place' algorithm [15], which randomly assigns positions and checks for overlaps. However, at higher volume fractions, repeated failures during overlap checks can cause infinite loops, preventing the desired fraction. To address this, the domain is divided into smaller sub-regions for localized placement, reducing computational complexity and improving efficiency. The ITZ, the weakest region in concrete, is modeled with a reduced bond strength to simulate early failure under loading, effectively weakening the interface. To study how aggregate shape affects drying shrinkage and cracking, the models were developed using regular polyhedra: hexahedron, octahedron, dodecahedron, and icosahedron, to represent aggregates and analyze the influence of sphericity of aggregate on cracking.

The concrete model, depicted in Fig. 2, is a cylinder measuring 9 mm in diameter and 18 mm in height. It includes spherical aggregates with a diameter of 3 mm, while aggregates of other shapes—regular polyhedra such as hexahedron, octahedron, dodecahedron, and icosahedron—are modeled with equivalent volumes. The model is discretized with uniform grid spacing of  $\Delta x = 0.2$  mm with 197088 material points. The horizon is set to  $\delta = 3.015\Delta x$ . The time step for the diffusion equation is specified as  $\Delta t = 0.1$  s. Aggregates are assumed to be elastic and impermeable in the simulation.

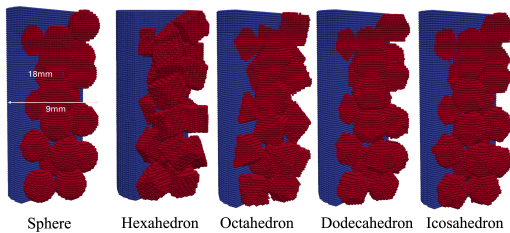


Figure 2: Meso-scale concrete model with aggregates of different shape

### 4.3 Simulations result of models with aggregates of various shapes

Sphericity, defined as the ratio of the volume of the largest inscribed sphere to the to-

tal volume of a particle, is a dimensionless geometric parameter that reflects the "roundness" of aggregates. Using sphericity to characterize aggregates is useful because it quantifies how closely the particles resemble a perfect sphere: higher values signify more spherical shapes. And the crack distribution in concrete samples was analyzed at various drying times:  $t=1800$  s (30 minutes),  $t=3600$  s (1 hour), and  $t=18000$  s (5 hours). By the 5-hour mark, the samples were fully dry, marking the end of the drying process.

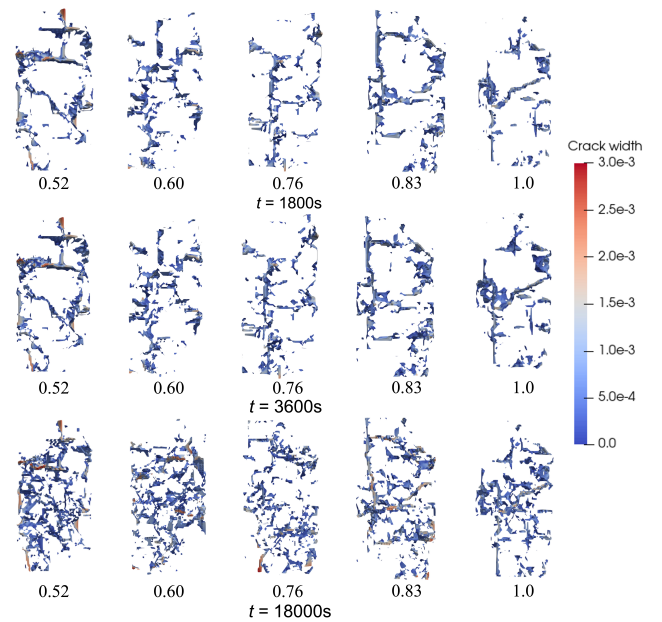


Figure 3: Distribution of cracks in samples with aggregates of varying sphericity at different drying times

As shown in Fig. 3, each drying stage revealed distinct differences in crack distribution for samples with varying aggregate sphericities. After 30 minutes, relatively wide fractures appeared on the concrete surface. By 1 hour, these surface cracks had grown wider and started penetrating into the sample interiors. At the end of the drying period, numerous narrow cracks developed within the concrete, especially around the aggregates. The arrangement of these interior cracks strongly depended on aggregate sphericity: as aggregates were more spherical, the occurrence of interior cracks diminished.

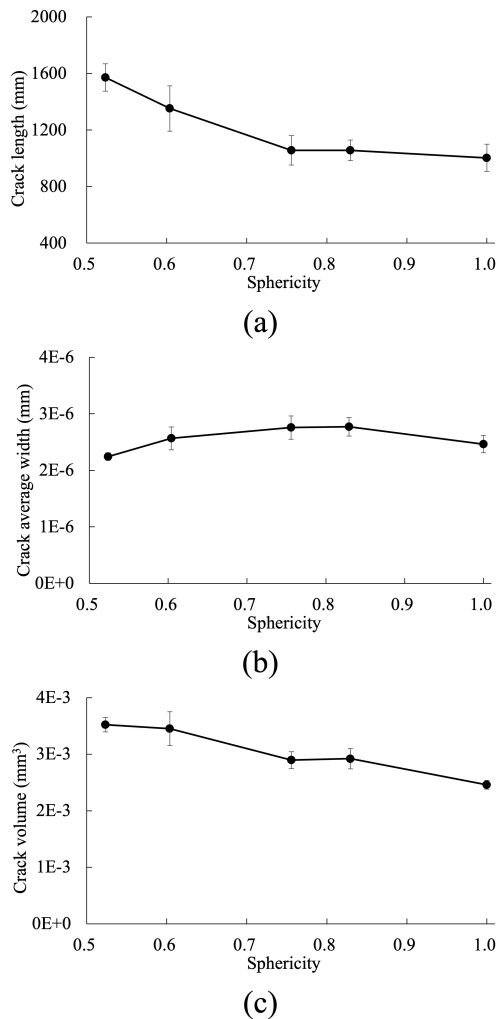


Figure 4: Crack information in samples with aggregates of varying sphericity: (a) Crack length ; (b) Crack average width; (c) Crack volume

To further explore the variations in cracking among the samples, we measured crack length, average crack width, and crack volume for each aggregate type. For statistical robustness, five concrete models were randomly generated for each type of aggregate. As shown in Figure 4 (a), crack length decreases markedly when sphericity increases from 0.5 to 1.0, dropping from about 1600 mm to roughly 1000 mm. This trend indicates that aggregates with higher sphericity lead to shorter cracks. Crack volume exhibits a similar decline, falling from  $4\text{E-}3 \text{ mm}^3$  to approximately  $2.5\text{E-}3 \text{ mm}^3$ , suggesting that more spherical aggregates reduce overall crack volume. The average crack width fluctuates between sphericity values of 0.5 and 0.8

but then gradually decreases as sphericity approaches 1.0, implying that greater sphericity tends to limit crack width. Overall, sphericity exerts a strong influence on crack development, with higher sphericity effectively minimizing crack length and volume, thereby enhancing the concrete's integrity during drying.

## 5 Conclusion

In this study, Peridynamic (PD) theory is utilized to develop a fully coupled hydro-mechanical BB-PD model for simulating meso-scale cracking in concrete aggregates. By constructing concrete models with aggregates of various shapes and modeling the drying process, the approach accurately captures crack formation and propagation induced by shrinkage. The analysis indicates that aggregate shape markedly influences crack behavior: higher sphericity promotes more uniform damage, shorter crack lengths, and fewer internal fractures, whereas lower sphericity concentrates damage, increases crack lengths, and leads to additional internal cracks. These findings highlight the importance of selecting aggregates with suitable shapes to mitigate drying shrinkage cracking, offering guidance for designing more durable and sustainable concrete mixtures.

## REFERENCES

- [1] Jamal A. Almudaiheem. Prediction of drying shrinkage of portland cement paste: Influence of shrinkage mechanisms. *Journal of King Saud University - Engineering Sciences*, 3(1):69–86, 1991.
- [2] M. P. Sez-Prez, M. Brmmer, and J. A. Durn-Surez. A review of the factors affecting the properties and performance of hemp aggregate concretes. *Journal of Building Engineering*, 31:101323, September 2020.
- [3] Zichao Pan, Rujin Ma, Dalei Wang, and Airon Chen. A review of lattice type model in fracture mechanics: theory, applications, and perspectives. *Engineering*

- Fracture Mechanics*, 190:382–409, March 2018.
- [4] P. Wang, N. Gao, K. Ji, L. Stewart, and C. Arson. DEM analysis on the role of aggregates on concrete strength. *Computers and Geotechnics*, 119:103290, March 2020.
- [5] Stewart A Silling. Reformulation of elasticity theory for discontinuities and long-range forces. *Journal of the Mechanics and Physics of Solids*, 48(1):175–209, 2000.
- [6] Liwei Wu, Dan Huang, Han Wang, Qipeng Ma, Xin Cai, and Junbin Guo. A comparison study on numerical analysis for concrete dynamic failure using intermediately homogenized peridynamic model and meso-scale peridynamic model. *International Journal of Impact Engineering*, 179:104657, 2023.
- [7] Maurice A Biot. General theory of three-dimensional consolidation. *Journal of applied physics*, 12(2):155–164, 1941.
- [8] M. Th. van Genuchten. A closed-form equation for predicting the hydraulic conductivity of unsaturated soils. *Soil Science Society of America Journal*, 44(5):892–898, 1980.
- [9] Yudan Jin, Meng Wang, Hailing Shi, Yun Jia, Qier Wu, Nicolas Burlion, and Jianfu Shao. Experimental and numerical study of the influence of inclusion size on the drying shrinkage cracking in cementitious composites. *International Journal for Numerical and Analytical Methods in Geomechanics*, 47(15):2762–2790, 2023.
- [10] Thomas Rougelot, Frédéric Skoczylas, and Nicolas Burlion. Water desorption and shrinkage in mortars and cement pastes: Experimental study and poromechanical model. *Cement and Concrete Research*, 39(1):36–44, 2009.
- [11] Xiangnan Qin, Chongshi Gu, Chenfei Shao, Xiao Fu, Luis Vallejo, and Yue Chen. Numerical analysis of fracturing behavior in fully-graded concrete with oversized aggregates from mesoscopic perspective. *Construction and Building Materials*, 253:119184, 2020.
- [12] Sadjad Naderi, Wenlin Tu, and Mingzhong Zhang. Meso-scale modelling of compressive fracture in concrete with irregularly shaped aggregates. *Cement and Concrete Research*, 140:106317, February 2021.
- [13] Lei Xu, Lei Jiang, Lei Shen, Lei Gan, Yijia Dong, and Chao Su. Adaptive hierarchical multiscale modeling for concrete trans-scale damage evolution. *International Journal of Mechanical Sciences*, 241:107955, 2023.
- [14] Hao Jin, Yuliang Zhou, and Chen Zhao. Mesoscale analysis of dry shrinkage fractures in concrete repair systems using fem and vem. *International Journal of Pavement Engineering*, 24(2):2144310, 2023.
- [15] Longfei Zhang, Xiaotong Sun, Hao Xie, and Jili Feng. Three-dimensional mesoscale modeling and failure mechanism of concrete with four-phase. *Journal of Building Engineering*, 64:105693, April 2023.